Pertanika J. Sci. & Technol. 30 (1): 691 - 708 (2022)

PERTANIKA JOURNALS

SCIENCE & TECHNOLOGY

Journal homepage: http://www.pertanika.upm.edu.my/

Dose Distribution of ^{192}Ir HDR Brachytherapy Source Measurement using Gafchromic® EBT3 Film Dosimeter and TLD-100H

Nor Shazleen Ab Shukor[1], Marianie Musarudin[1]*, Reduan Abdullah[2] and Mohd Zahri Abdul Aziz[3]

[1]School of Health Sciences, Universiti Sains Malaysia, Health Campus, 16150 USM, Kubang Kerian, Kelantan, Malaysia
[2]Hospital Universiti Sains Malaysia, 16150 USM, Kubang Kerian, Kelantan, Malaysia
[3]Advance Medical and Dental Institute, Universiti Sains Malaysia, 13200 USM, Kepala Batas, Penang, Malaysia

ABSTRACT

This study aims to measure the radial dose function $g(r)$ and anisotropy function $F(r, \theta)$ of High Dose Rate (HDR) ^{192}Ir source in a fabricated water-equivalent phantom using Gafchromic® EBT3 film and TLD-100H and to compare the results obtained with the MCNP5 calculated values. The phantom was fabricated using Perspex PMMA material. For $g(r)$, the EBT3 films with a required dimension and TLD-100H chips were placed at r=1, 2, 3, 5, and 10 cm from the source. The $F(r, \theta)$ measurements were carried out at r=1, 2, 3, 5, and 10 cm with the angle range from 10° to 170°. The result of $g(r)$ from EBT3 film and TLD-100H was in good agreement (2.10%±1.99). Compared to MCNP5, the differences are within 0.31% to 11.47% for EBT3 film and 0.08% to 10.58% for TLD-100H. For the $F(r, \theta)$, an average deviation with the MCNP5 calculation is 4.94%±2.7. For both $g(r)$ and $F(r, \theta)$, the effects are prominent at r=10 cm. At this distance, the response of both Gafchromic® EBT3 film and TLD-100H shows less sensitivity as the dose followed the inverse square law. This work demonstrates that Gafchromic® EBT3 film dosimeter and TLD-100H are suitable dosimeters in ^{192}Ir dosimetric measurements at a radial distance of <5 cm.

Keywords: ^{192}Ir brachytherapy source, dose distribution, Gafchromic® EBT3 film dosimeter, Monte Carlo simulation, TLD-100H dosimeter

ARTICLE INFO

Article history:
Received: 11 August 2021
Accepted: 21 October 2021
Published: 10 January 2022

DOI: https://doi.org/10.47836/pjst.30.1.37

E-mail addresses:
shazzleen@usm.my (Nor Shazleen Ab Shukor)
marianie@usm.my (Marianie Musarudin)
reduan@usm.my (Reduan Abdullah)
mohdzahri@usm.my (Mohd Zahri Abdul Aziz)
*Corresponding author

ISSN: 0128-7680
e-ISSN: 2231-8526

INTRODUCTION

Brachytherapy is an internal radiotherapy technique in which a sealed radiation source is placed inside or near the treated area. Iridium-192 (^{192}Ir) is the most frequent source used for HDR brachytherapy. The dose distribution around ^{192}Ir brachytherapy sources is inherently anisotropic and is characterised by steep dose gradients. As the dose gradient near radioactive sources is veer, the dose distribution in the surrounding tissues is difficult to be measured (Hsu et al., 2012). These properties had put a high demand on the dosimetry of ^{192}Ir brachytherapy source regarding the dosimeter's precision, size, and energy dependence (Kirisits et al., 2014). The American Association of Physicists in Medicine (AAPM) had introduced dose distribution parameters based on the direct dose distribution in a homogenous water medium in which the dose rate constant (Λ), the radial dose function $g(r)$, the geometry factor $G(r, \theta)$, and the anisotropy function $F(r, \theta)$ are the parameters in question (Chandola et al., 2010; Granero et al., 2011; Rivard et al., 2004).

Based on the literature, the most frequently reported dosimetry systems in the determination of the dosimetric function of ^{192}Ir source are film dosimetry and thermoluminescent dosimeter (TLD) (Ayoobian et al., 2016; Bassi et al., 2020; DeWerd et al., 2014; Sellakumar et al., 2009; Uniyal et al., 2011; Wu et al., 2014). The dosimetric functions of ^{192}Ir studied by Sellakumar et al. (2009) were measured the Λ , $g(r)$, and $F(r, \theta)$ for HDR ^{192}Ir source using Gafchromic® EBT films. Therefore, according to the findings, the Gafchromic® EBT film could be utilised to assess the brachytherapy dosimetric function as defined by the AAPM TG-43. Furthermore, another experimental study found that the TLD and Gafchromic® EBT2 film measured values for $F(r, \theta)$ are within 4% of each other (Uniyal et al., 2011).

A recent study by Bassi et al. (2020) reported, EBT3 film was energy independent and can be utilised for brachytherapy source dose monitoring despite being calibrated with a 6MV photon beam and could be expanded to be applied in clinical dosimetry brachytherapy. Besides film dosimetry, TLDs also was recommended for dosimetric measurement in brachytherapy because of their excellent sensitivity, miniature, flat energy response, and energy independence. However, according to a prior study, TLD's appropriateness for brachytherapy dosimetry was determined by high-precision measurements using some of the most regularly utilised brachytherapy sources (DeWerd et al., 2014). Apart from these dosimeters, Monte Carlo calculation has been reported as a reliable and preferable dosimetry system, and it is also commonly utilised in obtaining dosimetric data for brachytherapy sources (Patel et al., 2010).

Previously, dosimetry protocols or a set of dosimetry procedures employing film dosimetry and TLD had been published (Ayoobian et al., 2016; Bassi et al., 2020; Faghihi & Street, 2015; Palmer et al., 2013; Sellakumar et al., 2009). However, they reported the properties of Gafchromic EBT, EBT2 and TLD 100 in their study. On the other hand, the

dosimetric properties of the Gafchromic® EBT3 film and TLD-100H in brachytherapy dosimetry has not yet been clarified. Therefore, this study investigates the dose distribution of ^{192}Ir brachytherapy source for $g(r)$ and $F(r, \theta)$ in fabricated Perspex PMMA phantom using Gafchromic® EBT3 film dosimetry and TLD-100H and compared with dose distribution data obtained from MCNP5 calculated values.

MATERIALS AND METHODS

Nucletron ^{192}Ir MicroSelectron HDR Source

The Nucletron ^{192}Ir microSelectron HDR source (HDR, Nucletron Inc., The Netherlands) was modelled using MCNP5 code. The source has a material density, ρ of 22.56 g cm^{-3}, modelled with a 3.5 mm active length and 0.6 mm diameter (Wu et al., 2014). The cover used to enclose this source is stainless steel AISI 316L (ρ =8.027 g cm^{-3}) with a diameter of 1.1 mm. At the outer steel cover on the proximal side, a 5 mm AISI 304 stainless steel cable (ρ = 4.81 g cm^{-3}) extending from the cover was modelled in this calculation. The material compositions of these steel are as described by López et al. (2011). Figure 1 illustrates the detailed model of the source used in this study. The ^{192}Ir energy spectrum used in this study was adopted from the energy distribution described by Fazli et al. (2013). We have excluded the beta spectrum in the calculation due to its negligible contribution at >1 mm distance to the source.

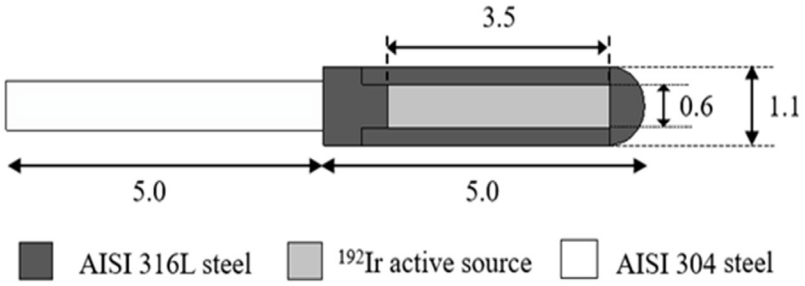

Figure 1. The geometry of Nucletron ^{192}Ir microSelectron HDR source modelled in MCNP5 calculation (length is in mm units)

Validation of the MCNP5 Dose Calculation

Identical simulation geometry defined by Wu et al. (2014) has been modelled using MCNP5 code, which is created by the Los Alamos National Laboratory (Los Alamos National Laboratory, Los Alamos, NM). This remodelling aims to compare and verify the dosimetric parameters obtained from our MCNP5 code. Therefore, a 30 cm spherical phantom filled

with homogeneous water (ρ=0.997 g cm^{-3}) was modelled. The $g(r)$ and $F(r,\theta)$ are the two dosimetric parameters considered for this purpose (Shukor et al., 2020). It is in line with the recommendation in AAPM TG-43,whereby the $g(r)$ is one of the most important dosimetric parameters for source validation and benchmarking (Rivard et al., 2004).

Fabricated Phantom Design

The phantom designed in this study was invented from a published study by Uniyal et al. (2011). A frequently used Perspex PMMA (polymethylmethacrylate) was selected as the phantom material due to the low effective atomic number (Z_{eff} = 6.5), economical, and widely available (de Almeida et al., 2002; Ghiassi-Nejad et al., 2001; Palmer et al., 2014; Subhalaxmi & Selvam, 2015). The Perspex PMMA slab phantom (ρ=1.19 g cm^{-3}) was fabricated at the Engineering Physic Workshop, School of Physic, USM (Figure 2).

The dimension of the Perspex PMMA phantom is 30×30×2 cm. This slab phantom has an inner diameter of 0.5 cm and was radially machined in the arced of 0° to 360° with a 1 to 10 cm distance from the centre. For TLD chips placement, the TLD holes were machined for 0.2 cm depth with 0.5 cm diameter at 1 to 10 cm radial distance with an angle of 10°, 30°, 60°, 90°, 120°, 150°, and 170°. In addition, a horizontal catheter insert was designed for source catheter delivery placement at the centre of the slab phantom.

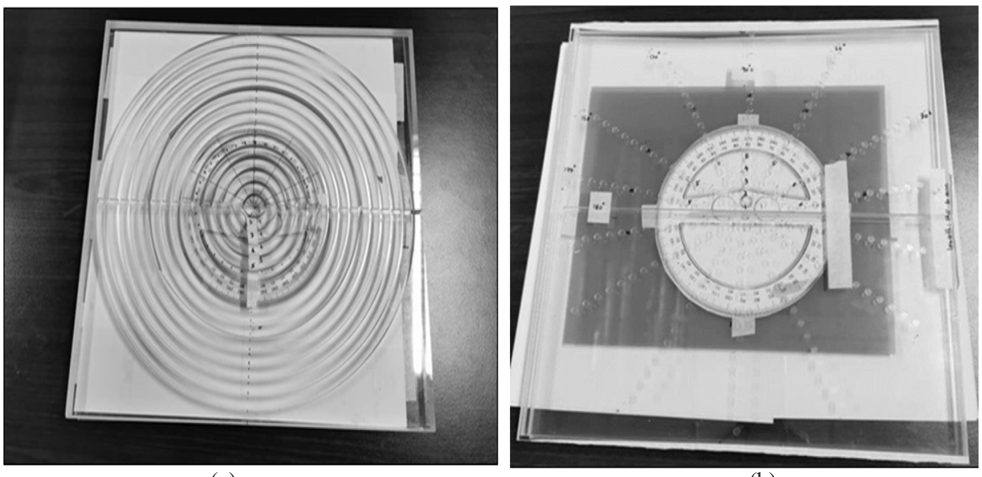

(a) (b)

Figure 2. The fabricated slab Perspex PMMA phantom for dose distribution measurement of ^{192}Ir brachytherapy source (a) with film inserts (b) with TLD holes

Dosimetry System

Radiochromic Film Dosimetry. The third-generation film, Gafchromic® EBT3 film (Ashland ISP, Wayne, NJ), is improved than their predecessor, EBT2, with features, such as symmetrical active layer configuration, with a dose range of 0.1-20 Gy and added matte polyester substrate, which has microscopic silica particles which keep minimising the gap thus preventing the formation of Newton's rings interference patterns (Fiandra et al., 2013; Reinhardt et al., 2012). With the new enhancement, EBT3 film was more robust and easier to handle than EBT2 (Borca et al., 2013; Reinhardt et al., 2012). Film lot #08231801 was used in this study and was handled according to the guidelines in the AAPM TG-55 (Niroomand-Rad et al., 2020).

The first phase of this study involved the calibration of the EBT3 film. As it is known as energy independent, the calibration is done with a 6MV photon beam (Adelnia & Fatehi, 2016; Palmer et al., 2013). A set of 10 pieces of EBT3 films were cut into 3×3 cm squares and marked at the left corner for orientation. For irradiation setup, the film pieces were placed in a full scatter solid water phantom at d_{max}=1.5 cm, and irradiation of 6MV photon beam was delivered with PRIMUS™ LINAC (Siemens Medical Systems, CA, USA) at SSD=100 cm, the field size of 10×10 cm and a dose range of 100 to 900 cGy. One sample was left unexposed as a background control for base and fog. After 24 hours of irradiation, the irradiated films were scanned in portrait orientation using 10000XL EPSON® Expression flatbed scanner (Epson Seiko Corporation, Nagano, Japan) with PTW-Filmscan software (PTW-Freiburg, Freiburg, Germany) with the setting parameters of positive colour film type, 16-bit grayscale, and 300 digital image resolutions (dpi) in a transmission mode (Figure 3). A curve between the pixel value and the corresponding dose was plotted from the PTW-Film Cal software v2.4 (PTW-Freiburg, Freiburg, Germany) (Figure 4). The film calibration curve was saved as a lookup table or calibration table for dose determination.

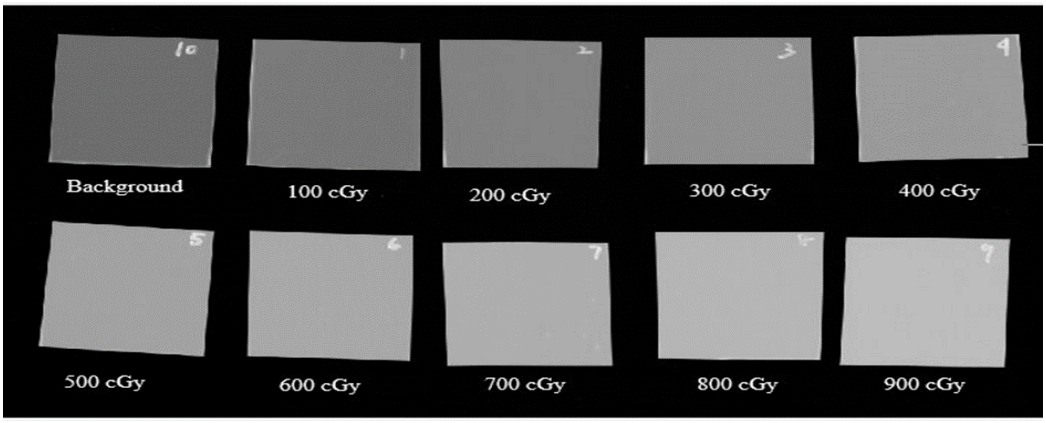

Figure 3. A set of Gafchromic® EBT3 films were digitalised using PTW-Filmscan software

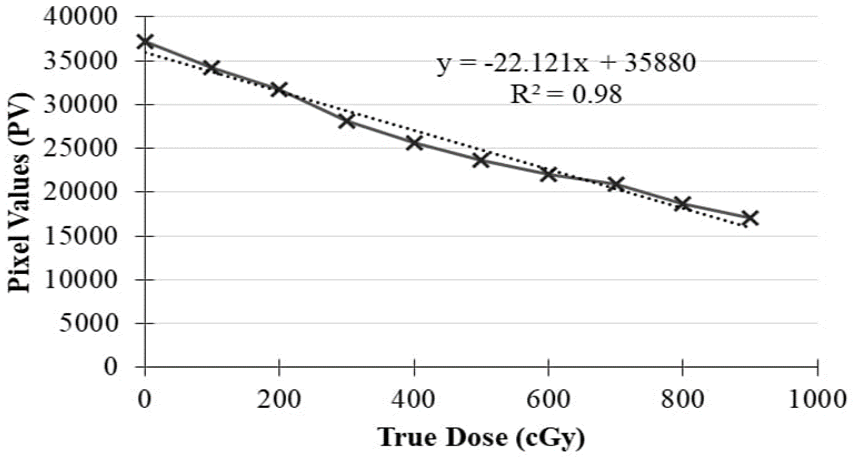

Figure 4. The dose-response of Gafchromic® EBT3 film generated by PTW- FilmCal software v2.4

Thermoluminescent Dosimeter (TLD) System

TLD measurements were performed with 3×3×1 mm chips of Harshaw TLD-100H (Thermo Fisher Scientific Inc., Waltham, MA). TLD100-H has been reported be to more sensitive, has a simple glow curve and short annealing than TLD100. As the brachytherapy source is known to have a steep dose gradient and will lose its energy in a short distance, it has been interesting to study the properties of TLD100-H towards the source (Freire et al., 2008). Therefore, the sensitivity test was performed by irradiating a group of 60 chips of TLD-100H with 100 cGy of 6MV photon beam using PRIMUS™ LINAC (Siemens Medical Systems, CA, USA) at SSD=100 cm, 10×10 cm field size, and d_{max}=1.5cm. The TL readout was performed 24 hours after irradiation using a Harshaw 3500 TLD reader (Thermo Fisher Scientific Inc. Waltham, MA).

The sensitivity factor for individual TLD is calculated using Equation 1.

$$Sensitivity = \frac{TLD_i}{TLD_{avg}} \quad [1]$$

Where, TLD_i is the individual reading of TLD and TLD_{avg} is the average reading. Since the response of individual TLD to the same delivered dose may be different, only the high sensitivity TLD chips with a sensitivity of >1 were used in this study. The reproducibility test was performed by repeating the same measurement three times. According to Faghihi & Street (2015), the calculation of the coefficient of variation (CV) of TLD measurement obtained using Equation 2 should be less than 10%.

$$CV\ (\%) = \frac{SD}{mean}\ x\ 100 \quad [2]$$

In addition, an individual Element Correction Coefficient (ECC) was also a required correction that needs to be applied. The characteristic of TL dosimeters could not present with the same TL efficiency (where TL efficiency (TLE) is defined as the emitted TL light intensity per unit of absorbed dose). Therefore, the ECC was calculated using Equation 3.

$$ECC_j = \frac{\langle TLE \rangle}{TLE_j} \quad [3]$$

Where, $<TLE>$ is the average reading of the total TLDs, whereas TLE_j is an individual reading. Calibration measurement was performed using 20 chips of TLDs with a CV of less than 10%, with the same setup that was used for the sensitivity test. The group calibration factor (CF) of TLD-100H is obtained by dividing the irradiated dose by the average response of the TLDs. From this study, the CF for this group of TLD-100H is 0.59 cGy/μC.

Radial Dose Function

The measurements setup was prepared by positioning the ^{192}Ir source inside the catheter at the centre of the Perspex PMMA slab phantom along the Y-axis with the tip of the source toward the +Y axis (Chandola et al., 2010). Before the exposure, source position verification to assess the source placement and a dwell position verification to keep the source at the centre of the film was performed. From the verification, the source position is confirmed to be centred on the field, and the dwell position is precisely placed in line at the centre of the 12.06 cm dwell length. Then. a set of films with the required dimension were placed in the film insert at radial distances (r) of 1, 2, 3, 5, and 10 cm from the source with the film facing toward the source at an angle of 90°. A full scattering medium was achieved by placing a Perspex PMMA slab with a thickness of 1 cm on the top of the fabricated phantom. The calculated source strength, *Sk* from the treatment planning, is 14911 cGy cm^{-2} h^{-1}. Referring to the *Sk*, the dwell time for completed 300 cGy is 72 s. The post-irradiated films were scanned after 24 hours using a 10000XL EPSON® Expression flatbed scanner (Epson Seiko Corp., Nagano, Japan) with a scanning parameter of 300 dpi and 16-bit grayscale. The film dose then was obtained from PTW-Verisoft software (PTW-Freiburg, Freiburg, Germany). The same irradiation setup also was performed for the TLD-100H measurements, which take place in the fabricated slab phantom with TLD holes as it has the same dimension as the slab phantom for a film. The signal readout was performed 24 hours' post-irradiation.

Anisotropy Function

The anisotropy function $F(r, \theta)$ describes the variation in dose distribution around the source as a function of polar angle relative to the transverse plane, including the effects of absorption and scatters in the medium due to; photon scattering in the medium,

self-filtration, and the primary photons' filtration through the encapsulation materials (Sellakumar et al., 2009). For the $F(r, \theta)$, the measurements were carried out using the same phantom as described for the $g(r)$. However, the dose values were measured at radial distances of 1, 2, 3, 5, and 10 cm with polar angles varied from 10° to 170°.

Monte Carlo Simulation

The dose distribution of the ^{192}Ir source was calculated using a validated MCNP5 code (Wu et al., 2014). The data were scored using an F6 tally grid system modelled by 0.5 mm height and ring radius of the cylindrical rings concentric from the source in its longitudinal axis. The concentric rings were positioned at r=0.5 to 14 cm from the centre, and they were fixed at the centre of the active length of the source in each calculation. The tip of the source was modelled to face towards the +Y direction while the cylindrical ring of the tally cells concentric to the Z-axis (Figure 5a). The data, which yielded at r=0.5 to 14 cm in the transverse plane of the source ($\theta = 90^{o}$), allows normalisation to the dose rate at r=1 cm of the same plane. Meanwhile, the data for $F(r, \theta)$ that measure doses at various angles from the source were tallied at a different angle from 0^{o} to 180^{o} with a 10^{o} increment. The centre of the active ^{192}Ir core was set as the centre of the angle rotation. The distal end of the stainless-steel cable was assumed as 0^{o}, while the tip end of the source is 180^{o} (Figure 5b).

The F6 tally calculates the amount of energy deposited in a unit of MeV/g. The output is multiplied by 1.6×10^{-10} using the tally multiplier (FM) card, yielding energy deposition in Gy. The photon cut-off was set at 10 keV to speed up the process (Shukor et al., 2020). A simulation boundary modelled by a 100 cm spherical cell was assigned to limit the simulation calculation. The radiation particles were removed from the calculation by force termination of the particles scattered out of the simulation boundary. The total number history of 5×10^{7} was selected to guarantee a reliable confidence interval <0.1.

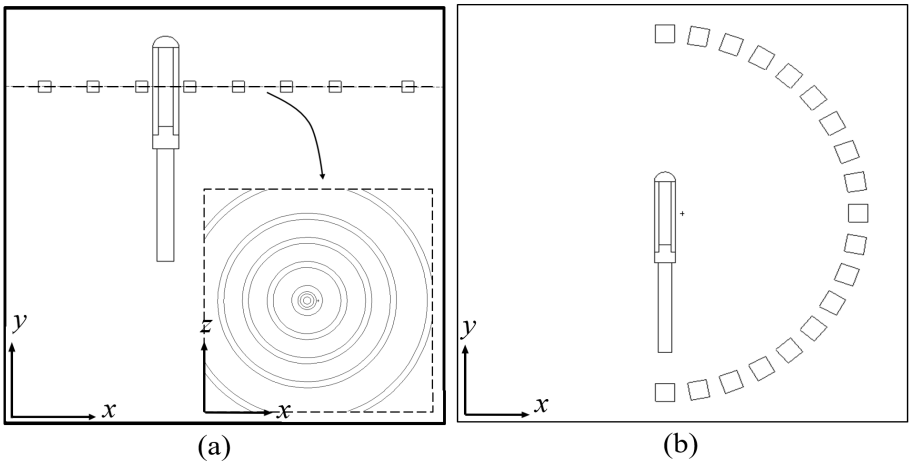

Figure 5. The geometry of the model was developed using MCNP5 code for (a) *g(r)* (b) $F(r, \theta)$

Dose Calculation Formalism

According to the AAPM TG-43 recommendation, the dose rate at the point of interest $P(r, \theta)$ in water is expressed as Equation 4:

$$D(r,\theta) = Sk\,\Lambda\,\frac{G\,(r,\,\theta)}{G(r_o,\theta_o)}.g(r).F(r,\theta) \quad [4]$$

Where, r is the distance (cm) from origin to the point of interest P, θ is the angle between the direction of radius vector r and the long axis of the source, θ_o defines the source transverse plane and is equal to π/2 radians, S_k is the air kerma strength, Λ is the dose rate constant, $G(r, \theta)$ is the geometry function, $g(r)$ is the radial dose function, and $F(r, \theta)$ is the anisotropy function. $P(r_0, \theta_0)$ is defined at r=1 cm, (θ = 90°)(Figure 6).

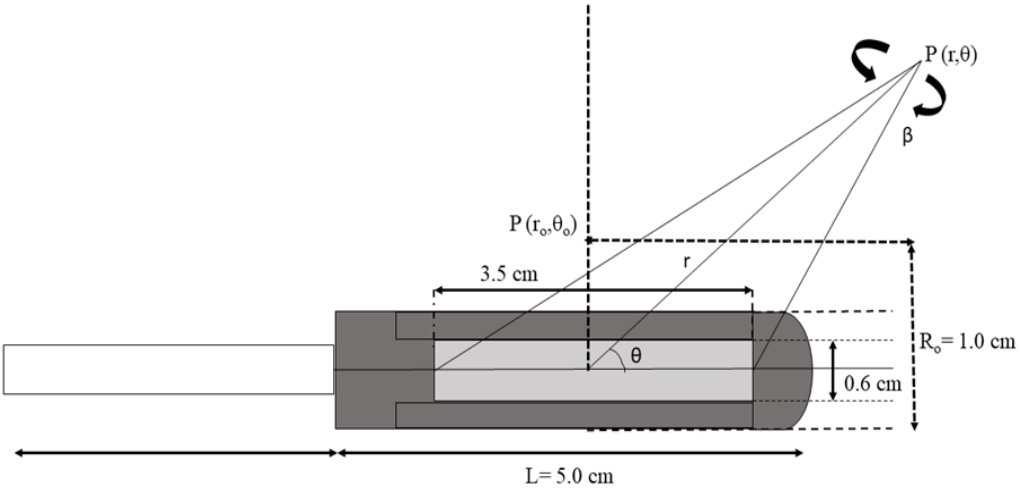

Figure 6. The geometry of line source used in TG-43 formalism

The Excel worksheet and formulas were used to simplify and calculate Equations 5, 6 and 7. The dose measured using TLD100-H and EBT3 film at a particular point has been inserted in the formula. The $g(r)$ is described as follows Equation 5:

$$g(r) = \frac{D(r,\ \theta_o)}{D(r_o,\ \theta_o)}.\frac{G(r_o,\ \theta_o)}{G(r,\ \theta_o)} \quad [5]$$

In this study, $g(r)$ was measured at a particular point using TLD100-H and EBT3 film. Where, dose at point, $D(r_0, \theta_0)$ is defined at 1 cm, θ=90º and $D(r, \theta_0)$ is defined at r=1, 2, 3, 4, 5 and 10 cm, θ=90º. The geometry function, $G(r, \theta)$ is calculated according to the following Equation 6:

$$G(r,\theta) = \frac{\beta}{Lr\sin\theta} \quad \text{if } \theta \neq 0^o \qquad [6]$$

Where, for $g(r)$ calculation, $G(r_0, \theta_0)$ is defined at r=1 cm, θ=90º and $G(r, \theta_0)$ is defined at r=1, 2, 3, 4, 5 and 10 cm, θ=90º. Whereas, L is the line source approximation used for the geometry function, β is the angle in radians, subtended by the tips of the hypothetical line source with respect to the calculation point $P(r, \theta)$.

The $F(r, \theta)$ is defined as in Equation 7:

$$F(r,\theta) = \frac{D(r,\ \theta)}{D\ r,\theta 0)} \cdot \frac{G\ (,r\ \theta 0)}{G(r,\ \theta)} \qquad [7]$$

Where, $D(r, \theta_0)$ is defined at r=1, 2, 3, 5 cm, θ=90º, $D(r, \theta)$ is defined at r = 1, 2, 3, 5 and 10 cm, θ=10º-170º, $G(r, \theta_0)$ is defined at r=1, 2, 3, 5 and 10 cm at θ=90º, $G(r, \theta)$ is defined at r=1, 2, 3, 5 and 10 cm at θ=10º-170°.

RESULTS AND DISCUSSION

Radial Dose Function

Figure 7 compared the measurement $g(r)$ of ^{192}Ir source using EBT3 film and TLD-100H with the calculated $g(r)$ by MCNP5 and published data previously presented by Wu et al. (2014). The average relative difference is 0.37% ±0.47, and a maximum deviation is at r=10 cm (1.30%). A previous study found that a good agreement is achieved when the deviation is within 2% (Buchapudi et al., 2019). Therefore, our MCNP5 code for the ^{192}Ir HDR brachytherapy dose calculation achieved a good agreement with Wu et al. (2014). We extended the simulation to r= 0.3, 0.5 and 0.7 cm and observed small deviations to the $g(r)$ at r=1 cm for the three radial distances (0.48, 0.12 and 0.01% each).

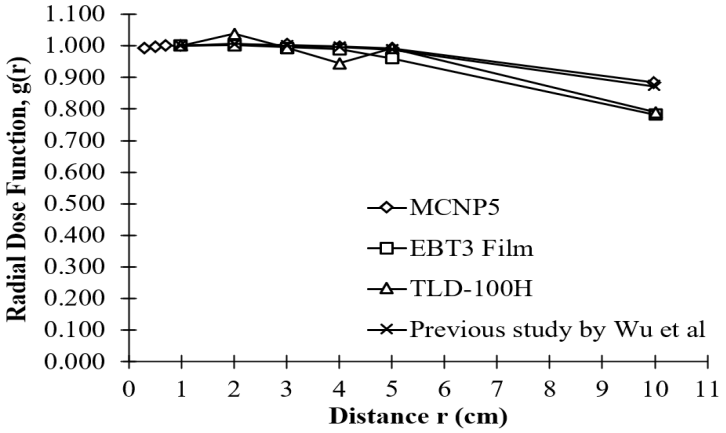

Figure 7. The comparison of measured, $g(r)$ for EBT3 film and TLD100-H with MCNP5 and a previous study by Wu et al. (2014)

Meanwhile, EBT3 film shows a good agreement with MCNP5 at r=1 to 5 cm with an average relative difference of 1.03%±1.25. However, a greater relative difference (11.47%) was calculated at r=10 cm. A similar result was observed for the TLD-100H whereby at r=1 to 5 cm, the $g(r)$ values were 1.92%±2.35. The maximum difference was also noted at r=10 cm (10.58%). Nevertheless, the experimental $g(r)$ values obtained between EBT3 film and TLD-100H were in good agreement with a relative difference of 2.10%±1.99. Even though a similar measurement setup was implemented for both film and TLD, slight variation was noted between the two, most probably due to the different dosimetry properties of film and TLD, e.g. differences in size, range of sensitivities, and measurement's principal (Uniyal et al., 2011). The $g(r)$ values between measured and calculated are within the tolerance at r=1 to 5 cm, and the differences are significant at r=10 cm. At this position, the response of TLD signal and film is relatively small, possibly because of the lower dose received due to the depth increase as mentioned in inverse square law (Hsu et al., 2012). In addition, the variation occurs because of the dose-response factor of the detector due to the shift of the photon spectrum to lower energies with increasing depth (Haworth et al., 2013).

Table 1

Comparison of the $g(r)$ measured using film in this study with the previous studies for a homogenous water phantom

Radial distance, r (cm)	**This study**	**Buchapudi et al.**	**Relative differences (%)**	**Sellakumar et al.**	**Relative differences (%)**
	EBT3	EBT2		EBT	
1	1.000	1.000	0.00	1.000	0.00
2	1.003	1.004	0.15	1.006	0.37
3	0.995	0.999	0.38	1.077	7.60
4	0.990	0.970	2.06	1.002	1.16
5	0.961	0.966	0.56	0.992	3.17
10	0.782	0.846	8.20	-	-
Relative Uncertainty (%)	3.5 (k=1)	2.4 (k=1)		1.5 (k=1)	

Table 2

Comparison of $g(r)$ measured using TLD in this study with the previous study for a homogenous water phantom

Radial distance, r (cm)	This study	Buchapudi et al.	Relative differences (%)
	TLD100-H	TLD100	
1	1.000	1.000	0.00
2	1.038	1.010	2.73
3	0.995	1.006	1.13
4	0.945	1.002	6.07
5	0.993	0.989	0.40
10	0.790	0.888	12.43
Relative uncertainty (%)	3.6 (k=1)	1.9 (k=1)	

Table 1 and Table 2 present the comparison between the measured $g(r)$ obtained in this study with the data previously presented by Buchapudi et al. (2019) and Sellakumar et al. (2009). From Table 1, the average relative difference between the film measurement with the previous studies is 1.89%±3.17 (Buchapudi et al., 2019) and 2.46%±3.12 (Sellakumar et al., 2009). Meanwhile, the comparison between the TLD measurements is shown in Table 2, whereby the relative difference between this study with Buchapudi et al. (2019) is 3.80%±4.77, with a maximum difference is at r=10 cm (12.43%). A significant difference was observed at r=10 cm, which is 8.20% and 12.43%, respectively. The disparities are probably due to the different phantom materials, dimensions, and the energy dependence of the detector at lower photon energies (Ghiassi-Nejad et al., 2001). Previous studies used EBT, EBT2 and TLD100 in their measurement. Our study shows that the performance of EBT3 film is lower than EBT and EBT2 (Fiandra et al., 2013). As TLD100-H is known to have higher sensitivity than TLD100, it suffers from a fluctuation from the thermal effect of Cu and P materials, which may degrade the TL sensitivity (Chen et al., 2002). Therefore, our measured $g(r)$ for film and TLD measurements are lower than the previous study but still within tolerance within <3.0% deviation. However, this may occur because of the

material of our Perspex PMMA phantom that was denser than water (ρ=1.19 g cm^{-3}), which caused higher attenuation than water, thus lowering the dose detected by the dosimeters (Sina et al., 2015).

Anisotropy Function

The measured $F(r, \theta)$ at radial distances of 1 cm, 2 cm, 3 cm, 5 cm, and 10 cm in a homogenous water medium is illustrated in Figures 8a-8e. Figure 8a shows the $F(r, \theta)$ at r=1 cm. Compared to the MCNP5 calculation, the average differences are 4.21% ±2.35 and 4.17%±3.74 for EBT3 film and TLD-100H, respectively. At $10° \leq \theta \leq 60°$, the difference was found to be at 4.46%±2.04 for film and 4.01%±1.20 for TLD. Meanwhile, at $120° \leq \theta \leq 170°$, the variation is at 5.38%±3.0 for EBT3 and 5.72%±4.54 for TLD-100H. The same trend was observed for r =2, 3, 5, and 10 cm (Figures 8b-8d). At r =5 cm (Figure 8d) and $10° \leq \theta \leq 60°$, the difference was found to be 6.44%±1.69 for EBT3 film and 6.74%±5.87 for TLD-100H. At the larger distance of r =10 cm (Figure 8e), the differences were 14.99%±5.81 for EBT3 film and 6.41%±3.50 for TLD-100H at $10° \leq \theta \leq 60°$. At a polar angle of $120° \leq \theta \leq 170°$, the variation is at 6.73%±5.87 for EBT3 and 5.37% ±2.27 for TLD-100H. The MCNP5 calculated $F(r, \theta)$ for r= 0.3, 0.5, 1.0 and 2.0 cm is shown in Figure 8f. As the $F(r, \theta)$ at r=0.3, 0.5, 1.0 and 2.0 cm at $30° < \theta < 120°$ is in a good agreement with the deviation range within 0.03%-0.86%, which is <1%. Meanwhile, at θ=180°, the deviation at r=0.3 cm (5.11%) and r=0.5 cm (2.1%), larger than r=2 cm (0.032%) The deviation for r <0.5 cm is larger due to the influence of dynamic internal components (DeWerd et al., 2011).

The deviation between the measured $F(r, \theta)$ and MCNP5 calculation is on the average of 4.94%. ±2.7. Similar to $g(r)$, the deviation may be caused by the different densities between water and Perspex PMMA. Figure 8 also show that the $F(r, \theta)$ values in the backward direction are non-symmetrical, possibly due to photon disruption by the drive wires and asymmetry in encapsulation thickness (Ghiassi-Nejad et al., 2001; Sellakumar et al., 2009). In addition, the geometric and activity distribution of the source modelled in MCNP5 simulations may differ from those in the actual distribution of source in EBT3 film and TLD-100H measurements. This minor variation may contribute to the large differences between the measured and calculated doses (Chiu-Tsao et al., 2014).

In comparison, the $F(r, \theta)$ values measured with EBT3 and TLD-100H show a good agreement with each other within 1.57%±1.21 at r=1 cm. The relative difference of $F(r, \theta)$ values between these is more prominent as the radial distance increases. The fluctuations occurred because of the effect of the air gap between the slab inserts in the Perspex PMMA phantom. The maximum discrepancy between EBT3 and TLD-100H was at 10.5%±7.85 at r=10 cm. This fluctuation is most probably due to the limited size of the TLD detector, which makes it challenging to obtain unperturbed dose values. As previously proved by Uniyal et al. (2011), diminishing the size of the detector exhibit some limitations related

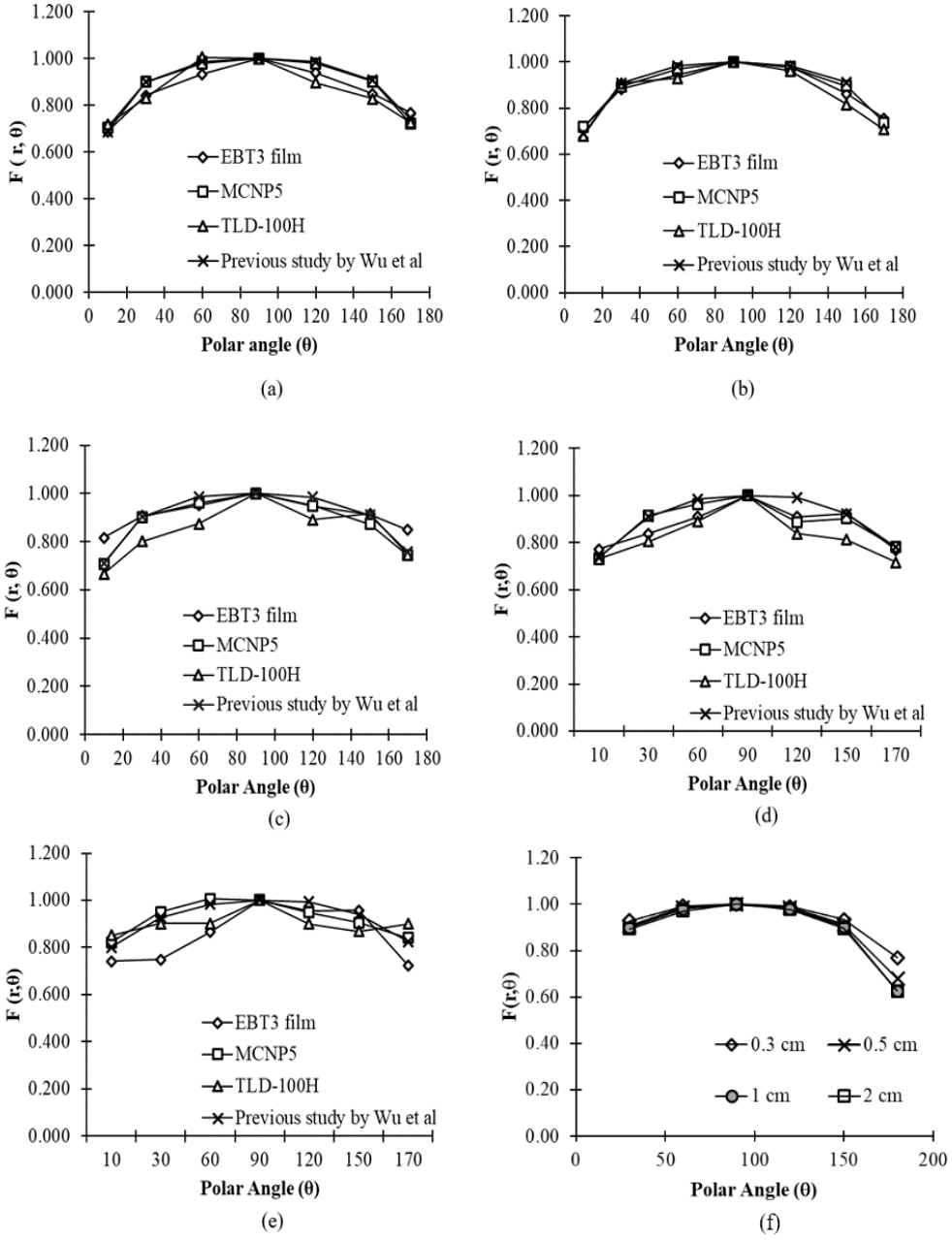

Figure 8. The measured and calculated of anisotropy function, $F(r, \theta)$ at radial distances of (a) 1 cm, (b) 2 cm, (c) 3 cm, (d) 5 cm, (e) 10 cm in a homogenous water medium and (f) 0.3, 0.5, 1 and 2 cm calculated using MCNP5

to the improper positioning of the phantom measurement accuracy. The EBT3 film utilised in this study provides a high spatial resolution. Therefore, the angular variation of $F(r, \theta)$ measured using EBT3 is expressed in a good response shape except for r=10 cm. At this distance, the response of both EBT3 film and TLD-100H shows less sensitivity in detecting the dose since the dose followed the inverse square law. Besides that, several factors, such as the probability of film scratches and dirt during the experiment handling, may also contribute to an error in the sensitivity of the EBT3 film and TLD-100H.

Uncertainty

The uncertainties of measurements and simulation results were calculated using NIST TN 1297. Type A uncertainty estimation is based on the standard error of the mean. For MCNP5, the relative uncertainty is 2.0% (k=1), TLD100-H is 3.6% (k=1), and for EBT3 measurement 3.5% (k=1). As recommended by the previous study, for low-and high-energy brachytherapy sources of low dose rate and high dose rate, a combined dosimetric uncertainty <5% (k=1) is estimated (DeWerd et al., 2011). The uncertainties between measured and simulations show a small difference but within tolerance for clinical practice.

CONCLUSION

This work demonstrates that Gafchromic® EBT3 film and TLD-100H are suitable dosimeters in ^{192}Ir dosimetric measurements at a radial distance of <5 cm. It was proved by a small average relative difference of $g(r)$ at r=1 to 5 cm between the measured and MCNP5, which is 1.03%±1.25 for EBT3 film and 1.92%±2.35 for TLD-100H. The $g(r)$ data obtained between TLD and film at r=1 to r=10 are in good agreement with each other within 2.10%±1.99. The deviation of measured $F(r, \theta)$ in the fabricated Perspex PMMA phantom with MCNP5 is 4.94%. For both parameters, the effects are prominent at a radial distance of r=10 cm with the maximum average difference of 11.47% for $g(r)$ and 14.99% for $F(r, \theta)$. At this distance, the response of both EBT3 film and TLD-100H shows less sensitivity as the dose followed the inverse square law. In addition, from the comparison between the older dosimeters, the performance of EBT3 film and TLD-100H does not show a significant difference between EBT2 and TLD100.

ACKNOWLEDGEMENT

Universiti Sains Malaysia supports the study under Short Term Grants number 304/PPSK/6315167.

REFERENCES

Adelnia, A., & Fatehi, D. (2016). Estimation and evaluation of tissue inhomogeneity effect on dose distribution for high dose rate iridium 192 source Using Monte Carlo simulation and film dosimetery. *Journal of Nuclear Medicine & Radiation Therapy, 7*(6), Article 1000312. https://doi.org/10.4172/2155-9619.1000312

Ayoobian, N., Asl, A. S., Poorbaygi, H., & Javanshir, M. R. (2016). Gafchromic film dosimetry of a new HDR 192Ir brachytherapy source. *Journal of Applied Clinical Medical Physics*, *17*(2), 194-205. https://doi.org/10.1120/jacmp.v17i2.6005

Bassi, S., Cummins, D., & McCavana, P. (2020). Energy and dose dependence of GafChromic EBT3-V3 film across a wide energy range. *Reports of Practical Oncology and Radiotherapy*, *25*(1), 60-63. https://doi.org/10.1016/j.rpor.2019.12.007

Borca, V. C., Pasquino, M., Russo, G., Grosso, P., Cante, D., Sciacero, P., Girelli, G., La Porta, M. R., & Tofani, S. (2013). Dosimetric characterization and use of GAFCHROMIC EBT3 film for IMRT dose verification. *Journal of Applied Clinical Medical Physics*, *14*(2), 158-171. https://doi.org/10.1120/jacmp.v14i2.4111

Buchapudi, R., Manickam, R., & Chandaraj, V. (2019). Experimental determination of radial dose function and anisotropy function of GammaMed plus 192Ir high-dose-rate brachytherapy source in a bounded water phantom and its comparison with egs-brachy Monte Carlo simulation. *Journal of Medical Physics*, *44*(4), 246-253. https://doi.org/10.4103/jmp.JMP_60_19

Chandola, R., Tiwari, S., Kowar, M., & Choudhary, V. (2010). Monte Carlo and experimental dosimetric study of the mHDR-v2 brachytherapy source. *Journal of Cancer Research and Therapeutics*, *6*(4), 421-426. https://doi.org/10.4103/0973-1482.77068

Chen, T. C., Stoebe, T. G., Horowitz, Y. S., & Oster, L. (2002). Role of impurities in the thermoluminescence of LiF:Mg,Cu,P. *Radiation Protection Dosimetry*, *100*(1-4), 243-246. https://doi.org/10.1093/OXFORDJOURNALS.RPD.A005857

Chiu-Tsao, S. T., Napoli, J. J., Davis, S. D., Hanley, J., & Rivard, M. J. (2014). Dosimetry for 131Cs and 125I seeds in solid water phantom using radiochromic EBT film. *Applied Radiation and Isotopes*, *92*, 102-114. https://doi.org/10.1016/j.apradiso.2014.06.014

de Almeida, C. E., Rodriguez, M., Vianello, E., Ferreira, I. H., & Sibata, C. (2002). An anthropomorphic phantom for quality assurance and training in gynaecological brachytherapy. *Radiotherapy and Oncology*, *63*(1), 75-81. https://doi.org/10.1016/S0167-8140(02)00065-8

DeWerd, L. A., Ibbott, G. S., Meigooni, A. S., Mitch, M. G., Rivard, M. J., Stump, K. E., Thomadsen, B. R., & Venselaar, J. L. M. (2011). A dosimetric uncertainty analysis for photon-emitting brachytherapy sources: Report of AAPM Task Group No. 138 and GEC-ESTRO. *Medical Physics*, *38*(2), 782-801. https://doi.org/10.1118/1.3533720

DeWerd, L. A., Liang, Q., Reed, J. L., & Culberson, W. S. (2014). The use of TLDs for brachytherapy dosimetry. *Radiation Measurements*, *71*, 276-281. https://doi.org/10.1016/j.radmeas.2014.05.005

Faghihi, R., & Street, M. (2015). Investigation of LiF, Mg and Ti (TLD-100) reproducibility. *Journal of Biomedical Physics & Engineering, 5*(4), 217-222.

Fazli, Z., Sadeghi, M., Zahmatkesh, M. H., Mahdavi, S. R., & Tenreiro, C. (2013). Dosimetric comparison between three dimensional treatment planning system, Monte Carlo simulation and gel dosimetry in nasopharynx phantom for high dose rate brachytherapy. *Journal of Cancer Research and Therapeutics, 9*(3), 402-409. https://doi.org/10.4103/0973-1482.119316

Fiandra, C., Fusella, M., Giglioli, F. R., Filippi, A. R., Mantovani, C., Ricardi, U., & Ragona, R. (2013). Comparison of Gafchromic EBT2 and EBT3 for patient-specific quality assurance: cranial stereotactic

radiosurgery using volumetric modulated arc therapy with multiple noncoplanar arcs. *Medical Physics, 40*(8), Article 082105. https://doi.org/10.1118/1.4816300

Freire, L., Calado, A., Cardoso, J. V, Santos, L. M., & Alves, J. G. (2008). Comparison of LiF (TLD-100 and TLD-100H) detectors for extremity monitoring. *Radiation Measurements*, *43*(2), 646-650. https://doi.org/https://doi.org/10.1016/j.radmeas.2007.12.013

Ghiassi-Nejad, M., Jafarizadeh, M., Ahmadian-Pour, M. R., & Ghahramani, A. R. (2001). Dosimetric characteristics of 192Ir sources used in interstitial brachytherapy. *Applied Radiation and Isotopes*, *55*(2), 189-195. https://doi.org/10.1016/S0969-8043(00)00375-4

Granero, D., Vijande, J., Ballester, F., & Rivard, M. J. (2011). Dosimetry revisited for the HDR brachytherapy source model mHDR-v2. *Medical Physics*, *38*(1), 487-494. https://doi.org/https://doi.org/10.1118/1.3531973

Haworth, A., Butler, D. J., Wilfert, L., Ebert, M. A., Todd, S. P., Hayton, A. J. M., & Kron, T. (2013). Comparison of TLD calibration methods for 192 Ir dosimetry. *Journal of Applied Clinical Medical Physics, 14*(1), 258-272. https://doi.org/10.1120/jacmp.v14i1.4037

Hsu, S. M., Wu, C. H., Lee, J. H., Hsieh, Y. J., Yu, C. Y., Liao, Y. J., Kuo, L. C., Liang, J. A., & Huang, D. Y. C. (2012). A study on the dose distributions in various materials from an Ir-192 HDR brachytherapy source. *PLoS ONE*, *7*(9), Article e44528. https://doi.org/10.1371/journal.pone.0044528

Kirisits, C., Rivard, M. J., Baltas, D., Ballester, F., De Brabandere, M., Van Der Laarse, R., Niatsetski, Y., Papagiannis, P., Paulsen Hellebust, T., Perez-Calatayud, J., Tanderup, K., Venselaar, J. L. M., & Siebert, F. A. (2014). Review of clinical brachytherapy uncertainties: Analysis guidelines of GEC-ESTRO and the AAPM q. *Radiotherapy and Oncology*, *110*, 199-212. https://doi.org/10.1016/j.radonc.2013.11.002

López, J. A., Donaire, J. T., & Alcalde, R. G. (2011). Monte Carlo dosimetry of the most commonly used 192 Ir high dose rate brachytherapy sources. *Revista de Física Médica*, *12*(3), 159-168.

Niroomand-Rad, A., Chiu-Tsao, S. T., Grams, M. P., Lewis, D. F., Soares, C. G., Van Battum, L. J., Das, I. J., Trichter, S., Kissick, M. W., Massillon-JL, G., Alvarez, P. E., & Chan, M. F. (2020). Report of AAPM Task group 235 radiochromic film dosimetry: An update to TG-55. *Medical Physics*, *47*(12), 5986-6025. https://doi.org/https://doi.org/10.1002/mp.14497

Palmer, A. L., Bradley, D. A., & Nisbet, A. (2014). Dosimetric audit in brachytherapy. *The British Journal of Radiology*, *87*(1041), Article 20140105. https://doi.org/10.1259/bjr.20140105

Palmer, A. L., Nisbet, A., & Bradley, D. A. (2013). Semi-3D dosimetry of high dose rate brachytherapy using a novel Gafchromic EBT3 film-array water phantom. *Journal of Physics: Conference Series*, *444*(1), Article 012101. https://doi.org/10.1088/1742-6596/444/1/012101

Patel, N. P., Majumdar, B., & Vijayan, V. (2010). Comparative dosimetry of GammaMed Plus high-dose rate 192Ir brachytherapy source. *Journal of Medical Physics, 35*(3), 137-143. https://doi.org/10.4103/0971-6203.66761

Reinhardt, S., Hillbrand, M., Wilkens, J. J., & Assmann, W. (2012). Comparison of Gafchromic EBT2 and EBT3 films for clinical photon and proton beams. *Medical Physics*, *39*(8), 5257-5262. https://doi.org/10.1118/1.4737890

Rivard, M. J., Coursey, B. M., DeWerd, L. A., Hanson, W. F., Huq, M. S., Ibbott, G. S., Mitch, M. G., Nath, R., & Williamson, J. F. (2004). Update of AAPM Task Group No. 43 Report: A revised AAPM protocol for brachytherapy dose calculations. *Medical Physics*, *31*(3), 633-674. https://doi.org/10.1118/1.1646040

Sellakumar, P., Sathish Kumar, A., Supe, S. S., Anand, M. R., Nithya, K., & Sajitha, S. (2009). Evaluation of dosimetric functions for Ir-192 source using radiochromic film. *Nuclear Instruments and Methods in Physics Research Section B: Beam Interactions with Materials and Atoms*, *267*(10), 1862-1866. https://doi.org/https://doi.org/10.1016/j.nimb.2009.03.003

Shukor, N. S. A., Musarudin, M., Abdullah, R., & Aziz, M. Z. A. (2020). Effects of different volumes of inhomogeneous medium to the radial dose and anisotropy functions in HDR brachytherapy. *Journal of Physics: Conference Series*, *1497*(1), Article 012027. https://doi.org/10.1088/1742-6596/1497/1/012027

Sina, S., Lotfalizadeh, F., Karimipourfard, M., Zaker, N., Amanat, B., Zehtabian, M., & Meigooni, A. S. (2015). Material-specific conversion factors for different solid phantoms used in the dosimetry of different brachytherapy sources. *Iranian Journal of Medical Physics*, *12*(2), 109-120. https://doi.org/10.22038/ijmp.2015.4774

Subhalaxmi, M., & Selvam, T. P. (2015). Phantom scatter corrections of radiochromic films in high-energy brachytherapy dosimetry: A Monte Carlo study. *Radiological Physics and Technology*, *8*(2), 215-223. https://doi.org/10.1007/s12194-015-0310-9

Uniyal, S. C., Naithani, U. C., & Sharma, S. D. (2011). Evaluation of Gafchromic EBT2 film for the measurement of anisotropy function for high-dose-rate 192Ir brachytherapy source with respect to thermoluminescent dosimetry. *Reports of Practical Oncology and Radiotherapy*, *16*(1), 14-20. https://doi.org/10.1016/j.rpor.2010.11.003

Wu, C. H., Liao, Y. J., Liu, Y. W. H., Hung, S. K., Lee, M. S., & Hsu, S. M. (2014). Dose distributions of an 192Ir brachytherapy source in different media. *BioMed Research International*, *2014*, Article 946213. https://doi.org/10.1155/2014/946213